Supplementary Information

A Thermo-Responsive MOF-Based H_2O_2-in-Oil "Pickering Emulsion In-Situ Catalytic System" for Highly Efficient Olefin Epoxidation

Bin Huang[a], Wei-Ling Jiang[b], Jie Han[c], Yan-Fei Niu[a], Hai-Hong Wu[a], and Xiao-Li Zhao[a]*

[a]Shanghai Key Laboratory of Green Chemistry and Chemical Processes, Department of Chemistry, East China Normal University, 3663 North Zhongshan Road, Shanghai 200062, P. R. China. Fax: 86-21-62233179; Email: *xlzhao@chem.ecnu.edu.cn.*

[b]Key Laboratory of Synthetic and Natural Functional Molecule of the Ministry of Education, College of Chemistry and Materials Science, Northwest University Xi'an 710127, P. R. China.

[c]Department of Science, School of Science and Technology, Hong Kong Metropolitan University, Hong Kong SAR, P. R. China.

General

^{1}H NMR and ^{31}P NMR spectra were obtained on a Bruker Avance-400 HD spectrometer with tetramethylsilane (TMS) as the internal standard. Fourier transform infrared (FT-IR) spectroscopy was conducted on a SHIMADZU IRTracer-100 spectrometer in the 500-4000 cm^{-1} range. Scanning electron microscopy (SEM) was conducted on a HITACHI S-4800 scanning electron microscope equipped with an energy-dispersive X-ray detector. The Powder X-ray diffraction (PXRD) patterns were recorded using a Rigaku (D/Max-Ultima IV)

diffractometer equipped with Cu *Kα* radiation (λ = 1.54184 Å). Confocal image was obtained on a NIKON A1R confocal fluorescence microscope. The aqueous phase was stained with fluorescein isothiocyanate (FITC) prior to the test and the emulsion was excited by a 488 nm laser. Dynamic light scattering (DLS) was conducted on a Malvern Zetasizer Nano ZS90 instrument. UV-visible spectroscopy was performed on a Shimadzu UV-2700 spectrophotometer. Inductively coupled plasma (ICP) measurement was performed on a Thermo IRIS Intrepid (II) XSP. The molecular weight was determined by gel permeation chromatograph (GPC, SHIMADZU RID-20A). X-ray photoelectron spectroscopy (XPS) data were obtained from AXIS SUPRA. Powders of MOFs were compressed into circular tablets using a table press (Shimadzu Press) for contact angle measurement. Water contact angle (WCA) was measured with the sessile drop method using a commercial contact angle analyzer (POWEREACH, JC2000C1). A droplet (2 μL) of DI water was deposited on the tablet in air using a precision syringe. The image was captured immediately after the droplet was deposited on the sample. Interfacial tension (IFT) in different temperature was measured on a high temperature and high pressure rotary drop interface tension meter (TX-500HP), using cyclohexane as the oil droplet with a rotation speed of 5000 r min^{-1}. For the aqueous phase, MOFs and PNIPAM were added into H_2O_2 at a concentration of 10 mg mL^{-1} and 1 mg mL^{-1}, respectively. Thermogravimetric analysis (TGA) was performed using a PerkinElmer STA 8000 in N_2 atmosphere in the temperature range of 30-800 ^oC and a heating rate of 10 ^oC min^{-1}. BET surface area and aperture size were measured by micromeritics ASAP 2020.

Characterization of series of MOFs and PNIPAM

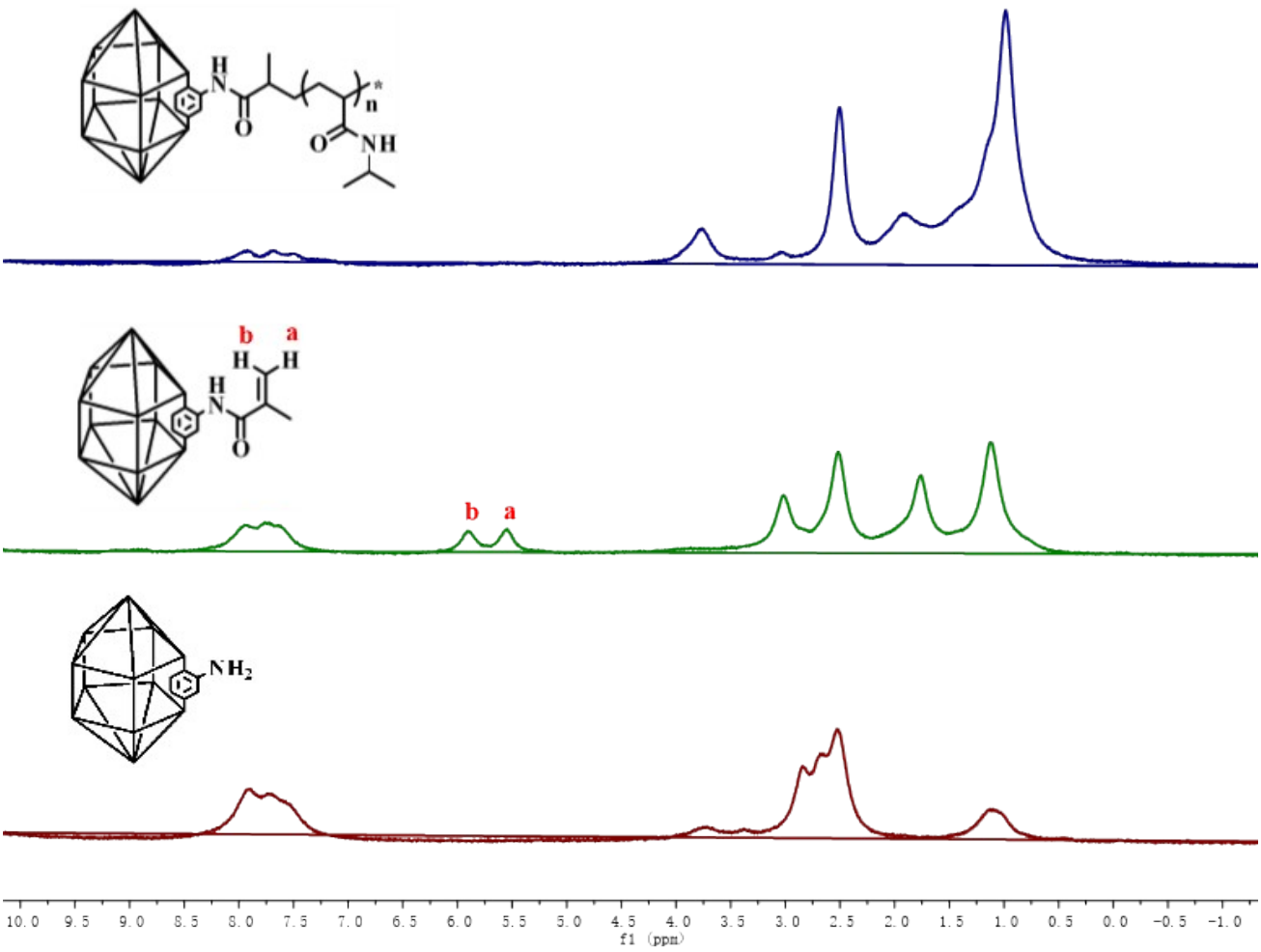

Figure S1. ^{1}H NMR (400 MHz, DMSO-d_6, 298 K) spectra of MIL-101-NH_2, MIL-101-NH-Met, and **MIL-101-NH-PNIPAM**.

Scheme S1 Synthesis of PNIPAM.

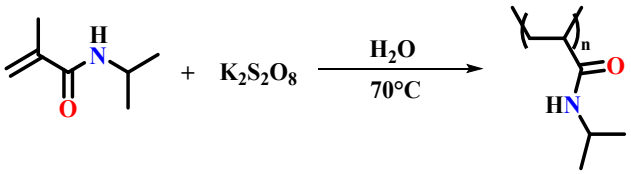

Synthesis of PNIPAM: Poly(N-isopropyl acrylamide) (PNIPAM) was prepared according to the literature method.[S1] Briefly, *N*-isopropyl acrylamide (NIPAM) monomer (1.13 g, 10 mmol) and DI water (20 mL) were added to a Schlenk flask and purged with high purity nitrogen in a dry ice bath for 15 min. The headspace of the flask was then purged with high purity nitrogen for 10 min. Then, potassium persulfate ($K_2O_8S_2$) (3.5 mg, 0.013 mmol) was weighed into a separate Schlenk flask and exposed to three vacuum and nitrogen purge cycles to remove the air. The NIPAM/deionized water solution was then transferred to the potassium persulfate flask via cannula and reacted for 72 h at 70 °C. The polymerization was quenched by rapid cooling upon immersion of the flask into liquid nitrogen. The synthesized polymer was precipitated in cold diethyl ether, and the precipitate was dried under vacuum at 80 °C overnight to afford a light-yellow powder of PNIPAM in 88 % yield. FTIR (KBr, cm^{-1}): 3279 (s), 2930 (m), 1767 (m), 1642 (s), 1504 (m), 1155 (m). ^{1}H NMR (DMSO-d_6, δ): (-CH_3, 1.04 ppm), (-CH, 3.87 ppm), (-(CH_2-CH-)-$_n$, 1.34-1.96 ppm).

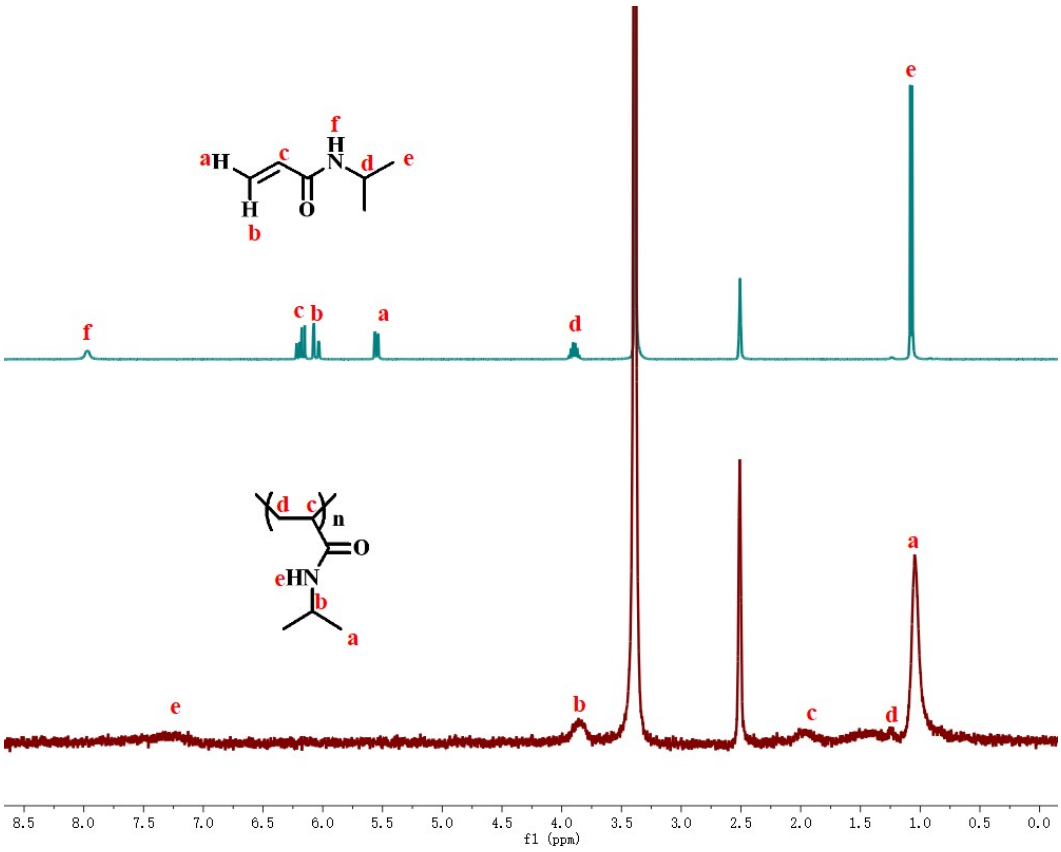

Figure S2. ^{1}H NMR (400 MHz, DMSO-d_6, 298 K) spectra of NIPAM and PNIPAM. Peaks at 3.39 ppm are assigned to H_2O

Table S1. The calculated molecular weight and dispersion index of PNIPAM, and the freed PNIPAM chains obtained by digesting **MIL-101-NH-PNIPAM** from GPC curves.

Specimen	*M*n	*M*w	*M*P	PDI
MIL-101-NH-PNIPAM	5386	5737	5583	1.26
PNIPAM	5911	6594	6468	1.12

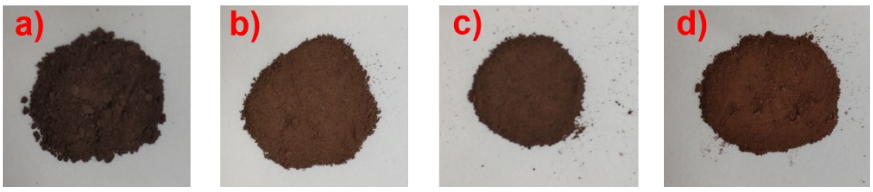

Figure S3. Visual images of (a) MIL-101-NH_2, (b) MIL-101-NH-Met, (c) **MIL-101-NH-PNIPAM** and (d) **NaPT@MIL-101-NH-PNIPAM**.

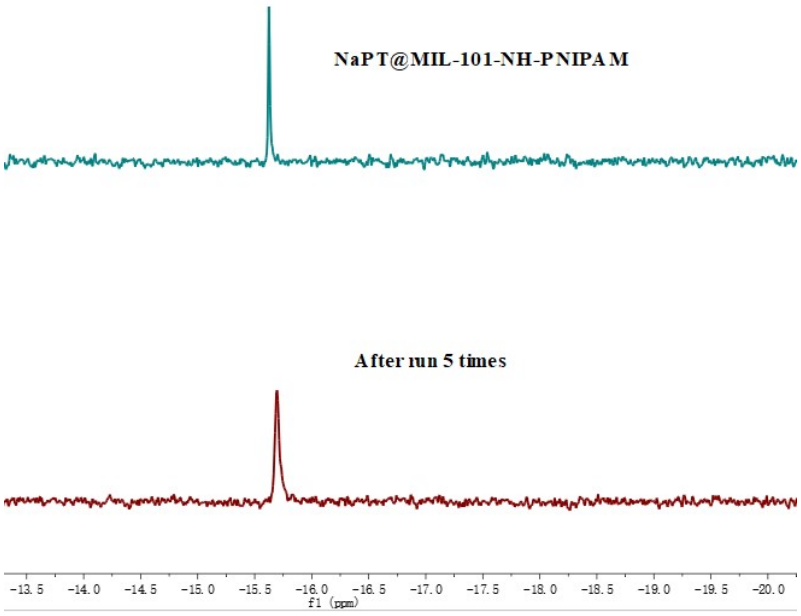

Figure S4. ^{31}P NMR (400 MHz, DMSO-d_6, 298 K) spectra of **NaPT@MIL-101-NH-PNIPAM** and after five runs.

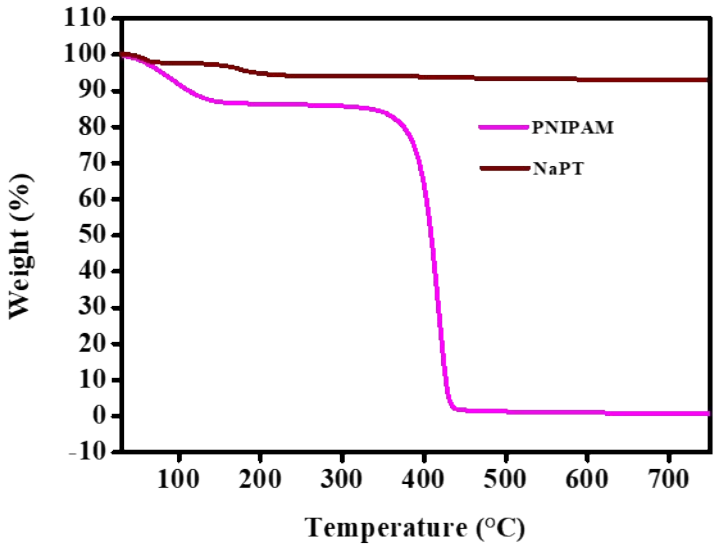

Figure S5. TGA curves of PNIPAM and NaPT in the range of 30 to 800 °C.

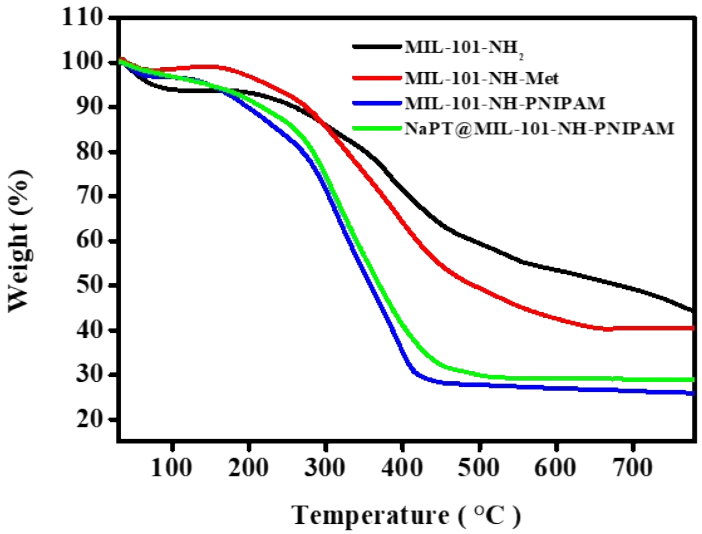

Figure S6. TGA curves of MIL-101-NH_2, MIL-101-NH-Met, **MIL-101-NH-PINIPAM** and **NaPT@MIL-101-NH-PINIPAM**, respectively.

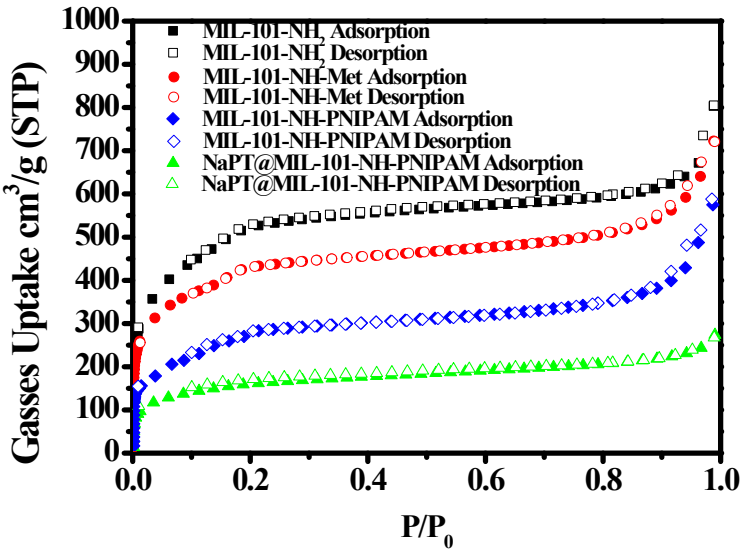

Figure S7. N_2 sorption isotherms of MIL-101-NH_2, MIL-101-NH-Met, **MIL-101-NH-PINIPAM** and **NaPT@MIL-101-NH-PINIPAM**, respectively.

Thermo-responsivity of series MOFs and PNIPAM

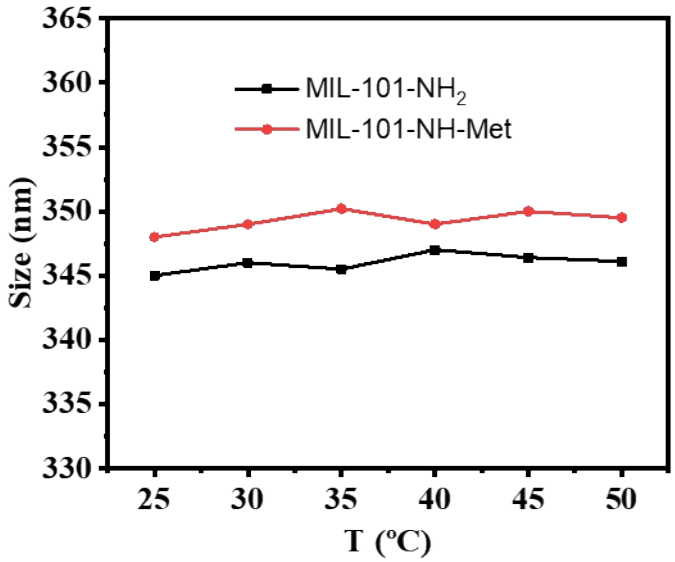

Figure S8. Hydrodynamic diameters of MIL-101-NH_2 and MIL-101-NH-Met in dilute aqueous solution of different temperatures.

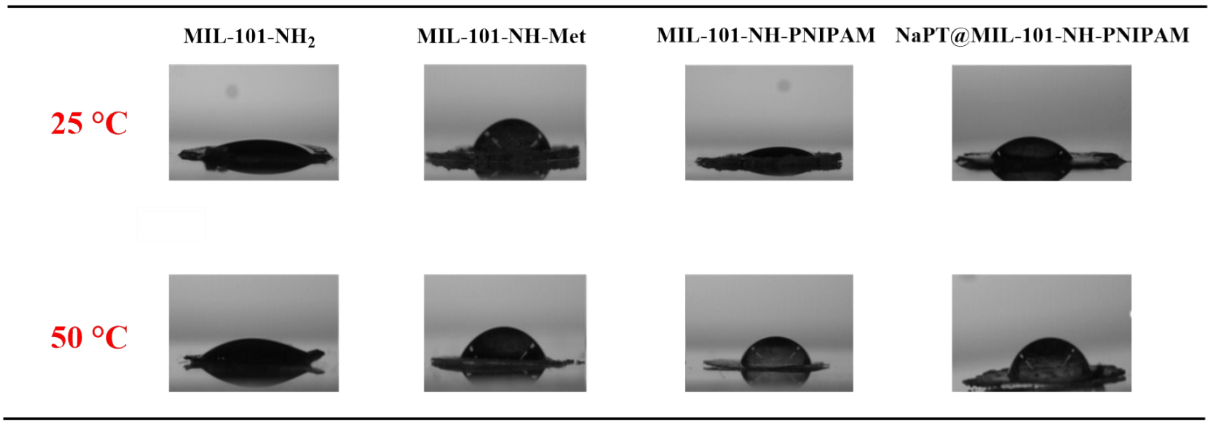

Figure S9. Water contact angles of MIL-101-NH_2, MIL-101-NH-Met, **MIL-101-NH-PINIPAM** and **NaPT@MIL-101-NH-PINIPAM** measured at different temperatures.

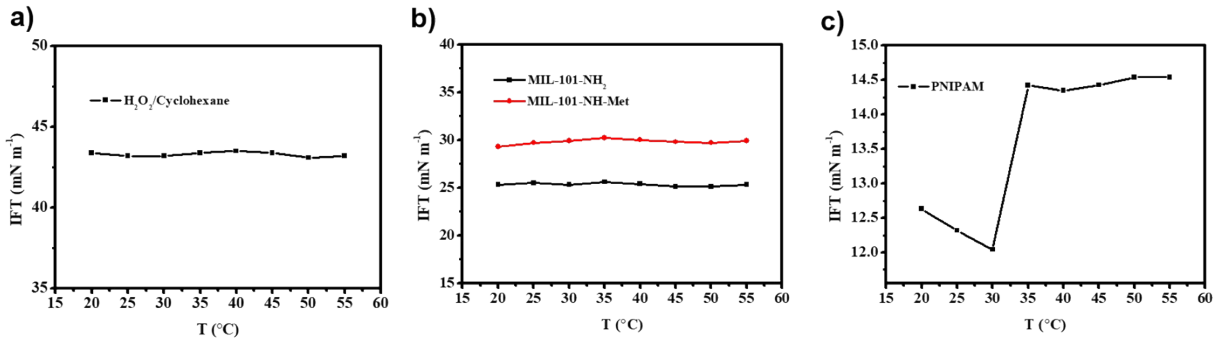

Figure S10. IFT data of (a) H_2O_2/cyclohexane; (b) MIL-101-NH_2 and MIL-101-NH-Met; (c) PNIPAM measured at different temperatures.

Characterization of MOFs-based Pickering emulsion

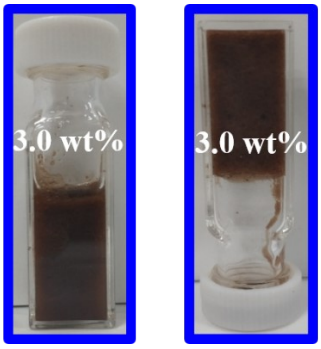

Figure S11. Visual images of the Pickering emulsion with 3.0 wt% **MIL-101-NH-PNIPAM** (cyclohexane-to-H_2O_2 = 2:1, v/v).

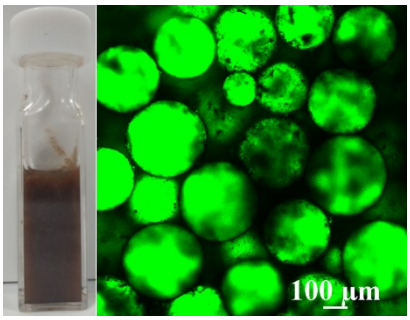

Figure S12. Visual and confocal microscopy images of **NaPT@MIL-101-NH-PNIPAM**-stabilized H_2O_2-in-cyclohexane Pickering emulsion after one week storage (2.0 wt%, cyclohexane-to-H_2O_2 = 2:1).

Thermo-responsivity of MOFs-based Pickering emulsion

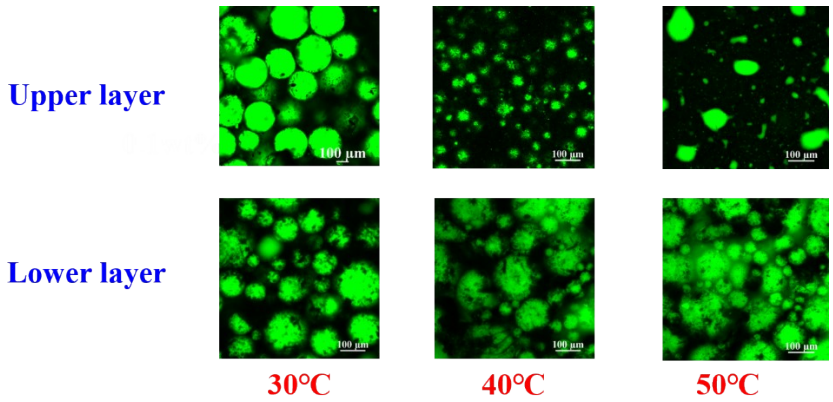

Figure S13. Confocal microscopy images of upper and lower layer of **NaPT@MIL-101-NH-PNIPAM** -stabilized Pickering emulsion (2.0 wt%, cyclohexane-to-H_2O_2 = 2:1, v/v) at 30, 40 and 50 ^oC, respectively.

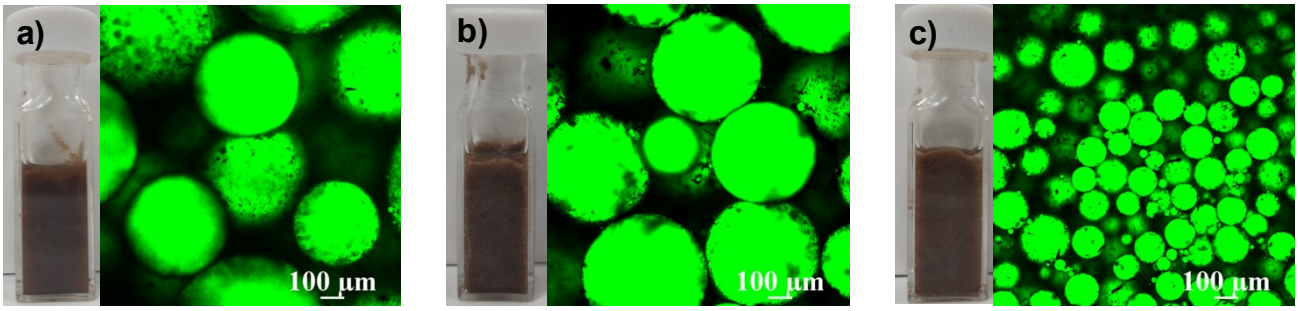

Figure S14. Visual images of the Pickering emulsion (with 2.0 wt% **MIL-101-NH-PNIPAM**) (a) *n*-pentane-to-H_2O_2 = 2:1, v/v; (b) *n*-hexane-to-H_2O_2 = 2:1, v/v; (c) toluene-to-H_2O_2 = 2:1, v/v.

Pickering emulsion in-situ catalytic system

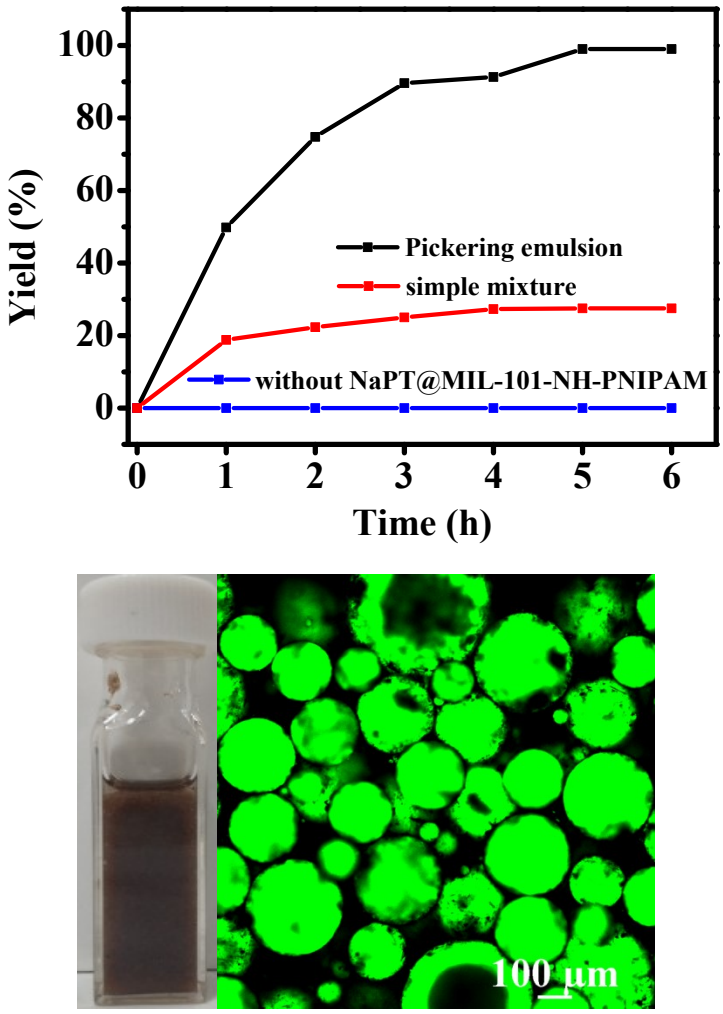

Figure S15. Catalytic performance in different systems (top); Visual and confocal microscopy images of **NaPT@MIL-101-NH-PNIPAM**-stabilized H_2O_2-in-cyclohexene&cyclohexane Pickering emulsion (2.0 wt%, cyclohexene&cyclohexane-to-H_2O_2 = 2:1, n(H_2O_2): n(cyclohexene) = 5:1) (bottom).

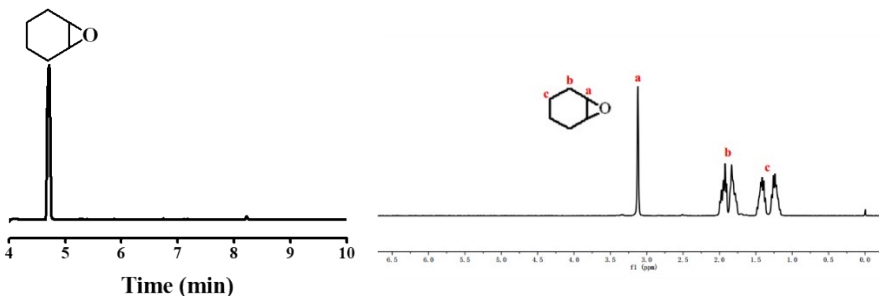

Figure S16. Left: GC spectra for the epoxidation reaction of cyclohexene catalyzed by **NaPT@MIL-101-NH-PNIPAM**-stabilized Pickering emulsion at 6.0 h. The conversion rate and selectivity are 99%, 99%, respectively. Right: ^{1}H NMR (300 MHz, $CDCl_3$, 298 K) spectra for the main product.

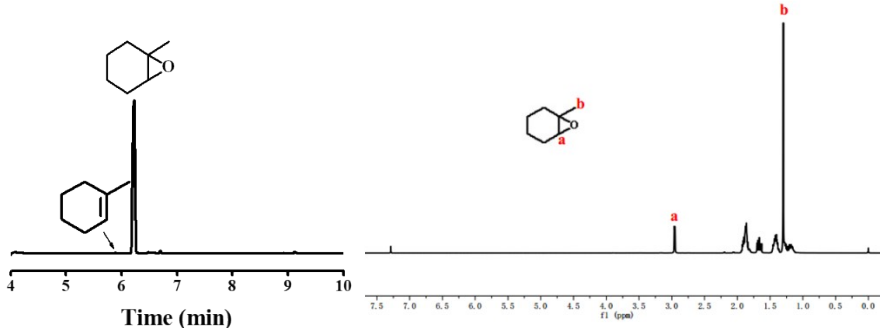

Figure S17. Left: GC spectra for the epoxidation reaction of 1-methyl-1-cyclohexene catalyzed by **NaPT@MIL-101-NH-PNIPAM**-stabilized Pickering emulsion at 8.0 h. The conversion rate and selectivity are 98%, 96%, respectively. Right: ^{1}H NMR (300 MHz, $CDCl_3$, 298 K) spectra for the main product.

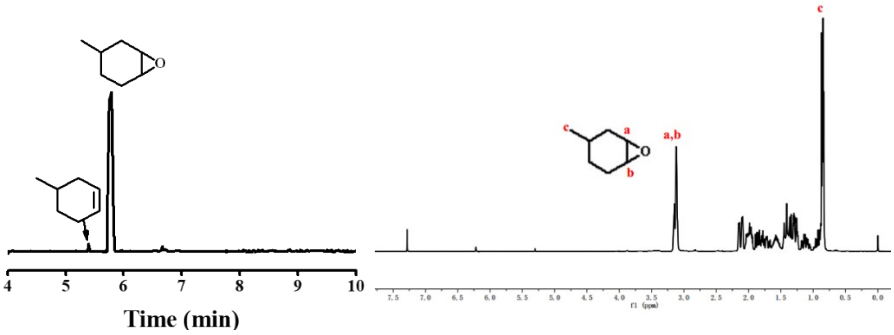

Figure S18. Left: GC spectra for the epoxidation reaction of 4-methyl-1-cyclohexene catalyzed by **NaPT@MIL-101-NH-PNIPAM**-stabilized Pickering emulsion at 6.0 h. The conversion rate and selectivity are 95%, 96%, respectively. Right: ^{1}H NMR (300 MHz, $CDCl_3$, 298 K) spectra for the main product.

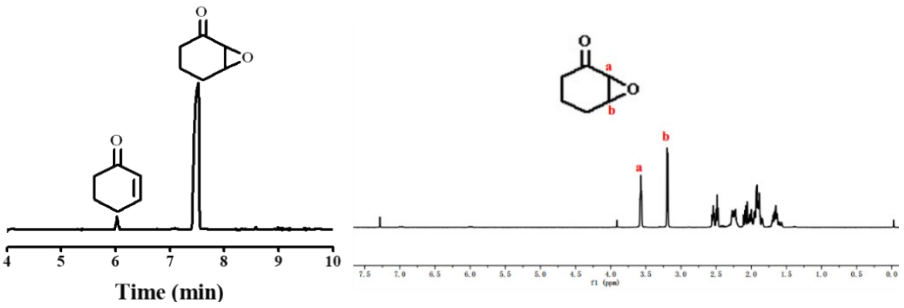

Figure S19. Left: GC spectra for the epoxidation reaction of 2-cyclohexen-1-one catalyzed by **NaPT@MIL-101-NH-PNIPAM**-stabilized Pickering emulsion at 6.0 h. The conversion rate and selectivity are 88%, 99%, respectively. Right: ^{1}H NMR (300 MHz, $CDCl_3$, 298 K) spectra for the main product.

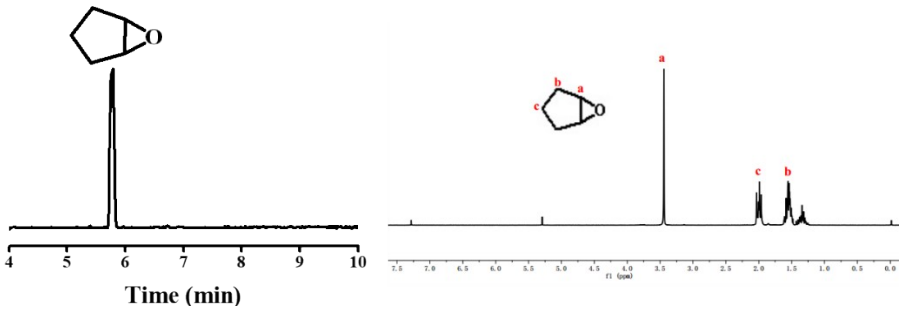

Figure S20. Left: GC spectra for the epoxidation reaction of cyclopentene catalyzed by **NaPT@MIL-101-NH-PNIPAM**-stabilized Pickering emulsion at 4.0 h. The conversion rate and selectivity are 99%, 99%, respectively. Right: ^{1}H NMR (300 MHz, $CDCl_3$, 298 K) spectra for the main product.

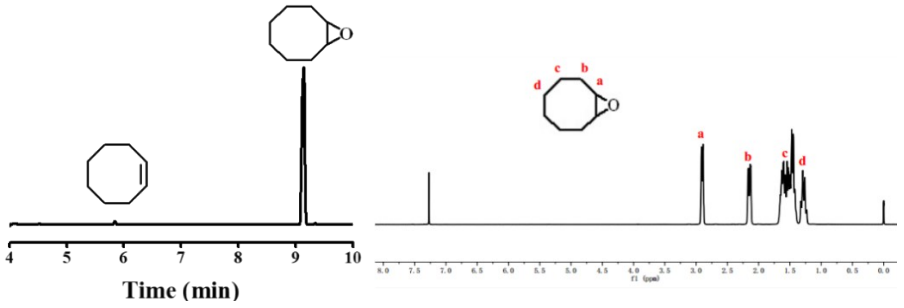

Figure S21. Left: GC spectra for the epoxidation reaction of cyclooctene catalyzed by **NaPT@MIL-101-NH-PNIPAM**-stabilized Pickering emulsion at 4 h. The conversion rate and selectivity are 96%, 97%, respectively. Right: ^{1}H NMR (300 MHz, $CDCl_3$, 298 K) spectra for the main product.

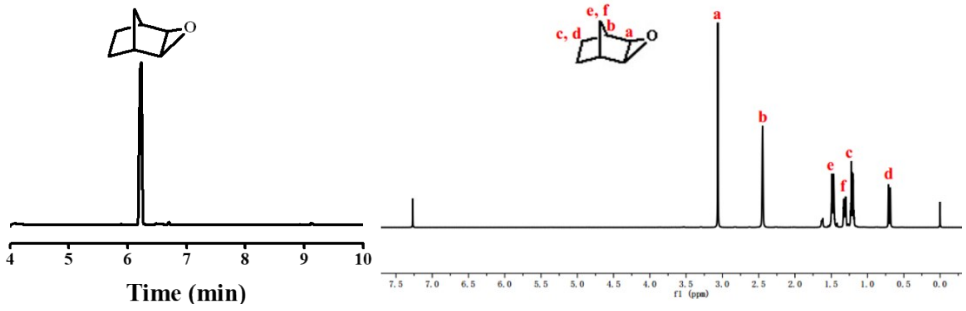

Figure S22. Left: GC spectra for the epoxidation reaction of norbornene catalyzed by **NaPT@MIL-101-NH-PNIPAM**-stabilized Pickering emulsion at 8.0 h. The conversion and selectivity are 97%, 99%, respectively. Right: ^{1}H NMR (300 MHz, $CDCl_3$, 298 K) spectra for the main product.

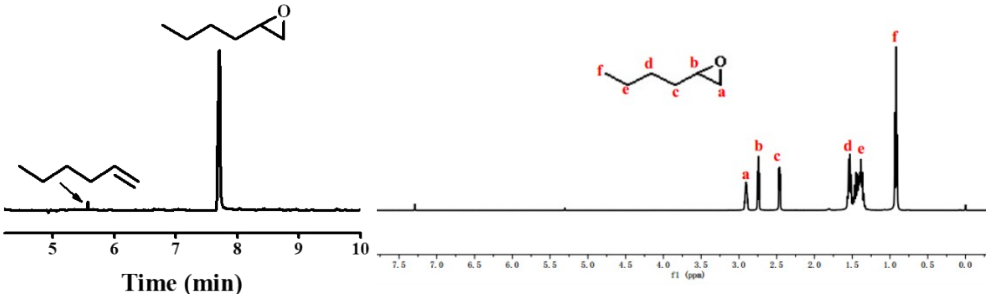

Figure S23. Left: GC spectra for the epoxidation reaction of 1-hexene catalyzed by **NaPT@MIL-101-NH-PNIPAM**-stabilized Pickering emulsion at 8.0 h. The conversion rate and selectivity are 95%, 97%, respectively. Right: ^{1}H NMR (300 MHz, $CDCl_3$, 298 K) spectra for the main product.

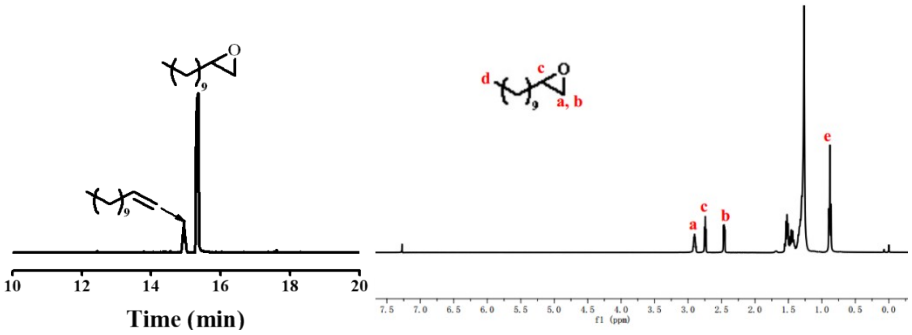

Figure S24. Left: GC spectra for the epoxidation reaction of propylene tetramer catalyzed by **NaPT@MIL-101-NH-PNIPAM**-stabilized Pickering emulsion at 10.0 h. The conversion rate and selectivity are 80%, 99%, respectively. Right: ^{1}H NMR (300 MHz, $CDCl_3$, 298 K) spectra for the main product.

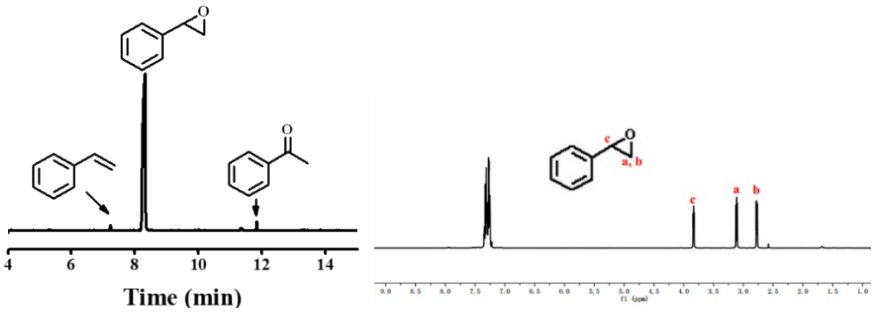

Figure S25. Left: GC spectra for the epoxidation reaction of styrene catalyzed by **NaPT@MIL-101-NH-PNIPAM**-stabilized Pickering emulsion at 10.0 h. The conversion and selectivity are 96%, 92%, respectively. Right: ^{1}H NMR (300 MHz, $CDCl_3$, 298 K) spectra for the main product.

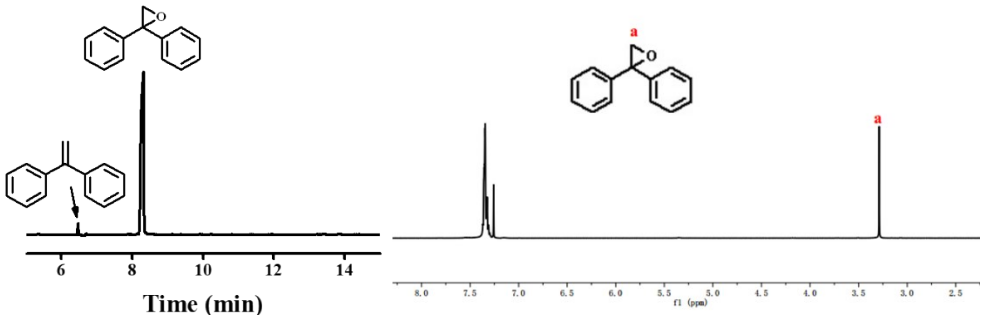

Figure S26. Left: GC spectra for the epoxidation reaction of 1,1-diphenylethylene catalyzed by **NaPT@MIL-101-NH-PNIPAM**-stabilized Pickering emulsion at 10.0 h. The conversion rate and selectivity are 95%, 99%, respectively. Right: ^{1}H NMR (300 MHz, $CDCl_3$, 298 K) spectra for the main product.

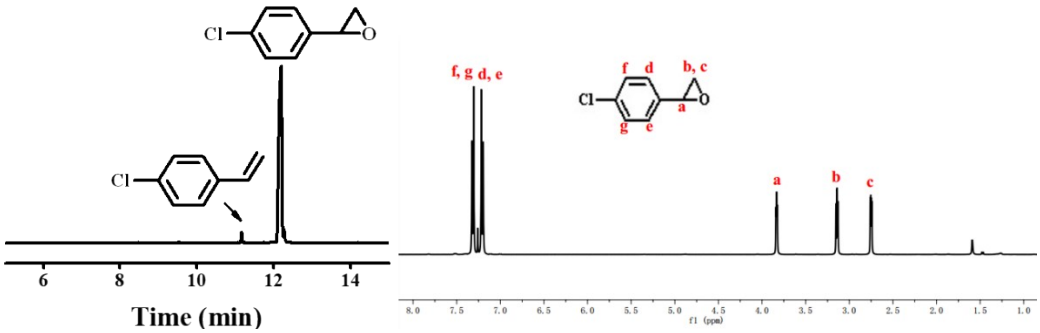

Figure S27. Left: GC spectra for the epoxidation reaction of 4-chlorostyrene catalyzed by **NaPT@MIL-101-NH-PNIPAM**-stabilized Pickering emulsion at 10.0 h. The conversion rate and selectivity are 95%, 99%, respectively. Right: ^{1}H NMR (300 MHz, $CDCl_3$, 298 K) spectra for the main product.

Table S2. Catalyst for olefin epoxidation reported in literatures (H_2O_2 as oxidant).

Catalyst	Reaction conditions	conversion (%)	Selectivity (%)	TOF[a] (h^{-1})
Ti-POM/MIL-101[17]	20 mg catalyst, 0.2 M H_2O_2, 50 °C, MeCN, 4 h	88	100	130
Ti-POM/MIL-101[17]	20 mg catalyst, 0.2 M H_2O_2, 50 °C, MeCN, 4 h	71	80	82
Ti-POM[17]	20 mg catalyst, 0.1 M H_2O_2, 50 °C, MeCN, 4 h	60	52	92
MIL-101[17]	20 mg catalyst, 0.1 M H2O2, 50 °C, MeCN, 4 h	40	41	
CoPMA@UiO-bpy[S2]	10 mg catalyst, 2 M H_2O_2, 70 °C, MeCN, 6 h	91	>99	
PMA@UiO-bpy[S2]	10 mg catalyst, 2 M H_2O_2, 70 °C, MeCN, 6 h	80	>99	
CoPMA@UiO-67[S2]	10 mg catalyst, 2 M H_2O_2, 70 °C, MeCN, 6 h	82	>99	
PMA@UiO-67[S2]	10 mg catalyst, 2 M H_2O_2, 70 °C, MeCN, 6 h	75	>99	
CoPMA/POP-II[S2]	10 mg catalyst, 2 M H_2O_2, 70 °C, MeCN, 9 h	79	>99	
PMA/KAP[S2]	10 mg catalyst, 2 M H_2O_2, 70 °C, MeCN, 9 h	26	>99	
poly(N-isopropylacrylamide)-derived polymer-$PW_{12}O_{40}$[3]	0.02 M% catalyst, 30% H_2O_2 (5.05 mmol), r.t., 13 h	73~99		
DIM–CIM–PW[2]	6 M% catalyst, 30% H_2O_2 (12 mmol), 60 °C, 6 h	100	100	
DIM–PW[2]	6 M% catalyst, 30% H_2O_2 (12 mmol), 60 °C, 6 h	4	100	
CIM–PW[2]	6 M% catalyst, 30% H_2O_2 (12 mmol), 60 °C, 6 h	10	100	
DIM-CIM-$PW_{12}O_{40}$[2]	6 M% catalyst, 30% H_2O_2 (12 mmol), 60 °C, 6 h	12	95	
TiMecapSBA15-O_2[8]	35 mg catalyst, 30% H_2O_2 (0.62 ml), 65 °C, 2~24 h		37~45	
(CH_3CO)capTiMecapSBA15[8]	35 mg catalyst,		38~49	

	30% H_2O_2 (0.62 ml), 65 °C, 2~24 h			
(CF_3CO)capTiMecapSBA15[8]	35 mg catalyst, 30% H_2O_2 (0.62 ml), 65 °C, 2~24 h		58~71	
Ga_2O_3-NR[10]	40 mg of catalyst， 4 mmol H_2O_2, ethyl acetate, 80 °C, 4 h	84	>99	
γ-Ga_2O_3-lit[10]	40 mg of catalyst， 4 mmol H_2O_2, ethyl acetate, 80 °C, 4 h	14	>99	

[a] TOF = (moles of substrate consumed)/[(moles of catalyst) × time]; determined from the initial rates.

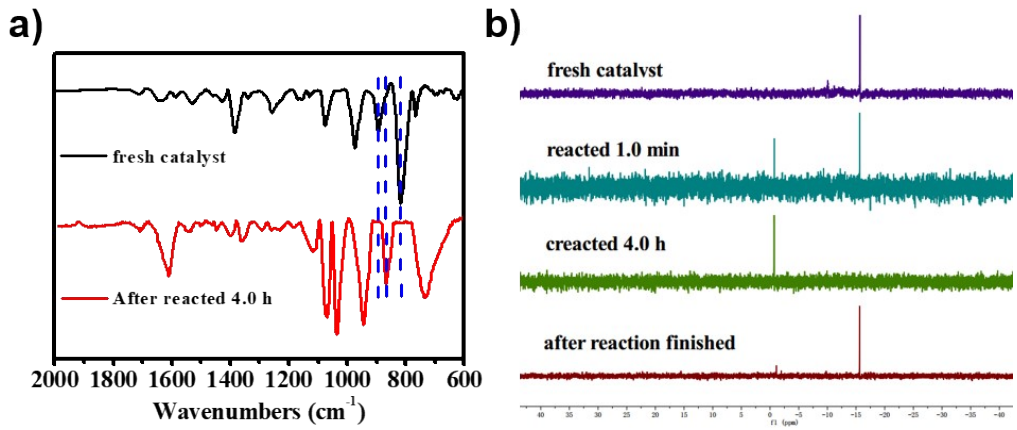

Figure S28. (a) IR spectra of **NaPT@MIL-101-NH-PINIPAM** before and after 4 hours. (b) ^{31}P-NMR (400 MHz, $CDCl_3$, 298 K) spectra of **NaPT@MIL-101-NH-PINIPAM** before and after reacted for a period of time (1.0 minutes, 4.0 hours, after reaction finished).

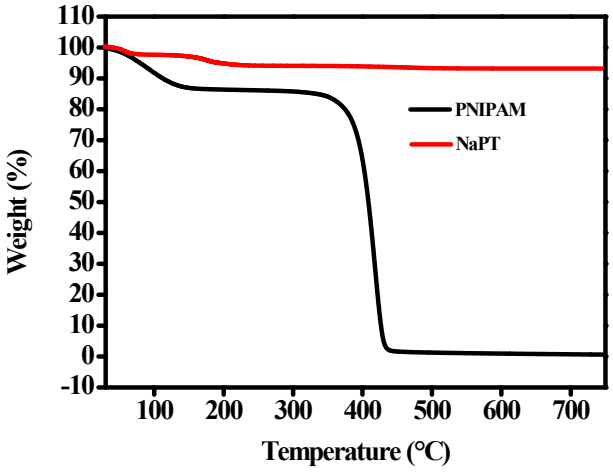

Figure S29. TGA curves of **NaPT and PNIPAM** after they were used for 4 hours.

A possible catalytic mechanism was proposed: when the **NaPT@MIL-101-NH-PNIPAM** was treated with H_2O_2, a new peak appeared at 863 cm^{-1} for the peroxo-oxygen band v(O-O), meanwhile, 896 for W-Ob-W and 817 cm^{-1} for W-Oc-W disappeared, indicating that the corner top shared oxygen and the co-edge bridging oxygen broke (Fig. S28a). It is attributed to the peroxo-oxygen in peroxo-tungsten species $[PO_4\{WO(O_2)_2\}_4]^{3-}$, which has been known as the active species for H_2O_2-based epoxidations. [S3] When H_2O_2 was completely converted to H_2O, $[PO_4\{WO(O_2)_2\}_4]^{3-}$ was converted to $[PW_{12}O_{40}]^{3-}$. We could also find the corresponding changes in ^{31}P-NMR. When the reaction was carried out for 4 hours, a new peak appeared at -0.709 ppm (Fig. S28b), which belongs to $[PO_4\{WO(O_2)_2\}_4]^{3-}$, and the peak at -15.623 ppm disappeared, which belongs to $[PW_{12}O_{40}]^{3-}$. When the reaction was over, the peak at -15.623 ppm appeared again, indicated that the H_2O_2 was exhausted. In addition, from the TGA traces, the overall structure of SPT did not change before and after being treated with H_2O_2 (Fig. S29).

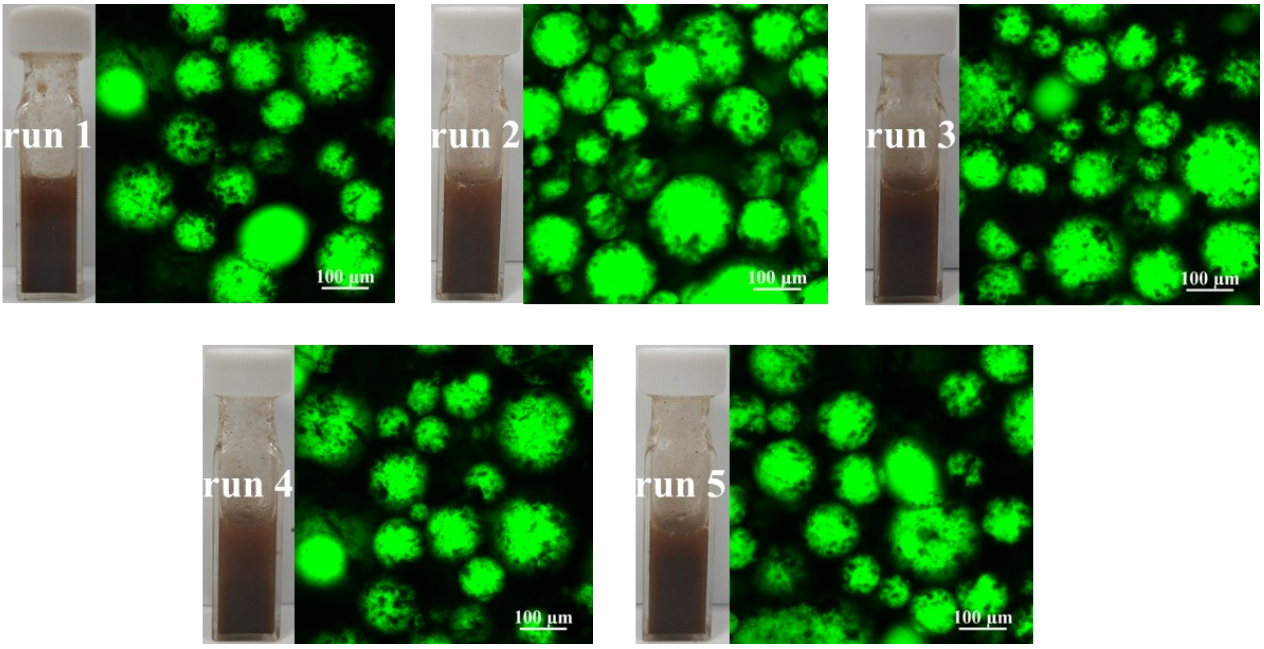

Figure S30. Confocal microscopy images of **NaPT@MIL-101-NH-PNIPAM**-stabilized Pickering emulsion after each catalytic run.

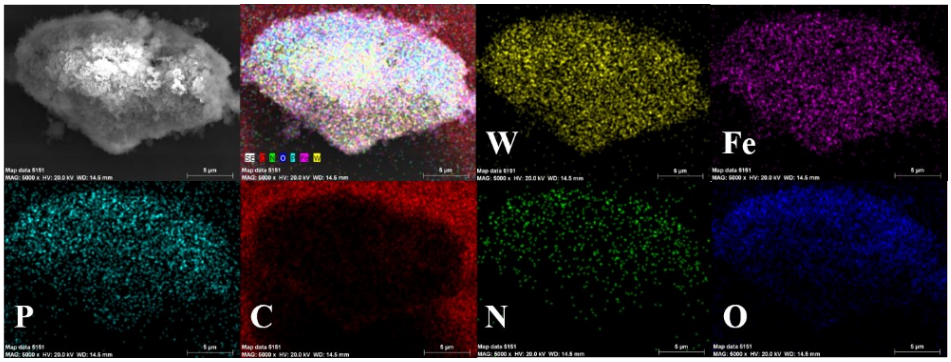

Figure S31. SEM-EDX images of **NaPT@MIL-101-NH-PNIPAM** after three runs.

Table S3. Abbreviation of the sample names in the manuscript.

Samples	Abbreviation
Methacrylamide group decorated MIL-101-NH-MOF NPs	MIL-101-NH-Met
Poly(*N*-isopropyl acrylamide) brushes-tethered MIL-101-NH-MOF NPs	**MIL-101-NH-PNIPAM**
Sodium phosphotungstate	NaPT
NaPT particles loaded MIL-101-NH MOF particles	**NaPT@MIL-101-NH-PNIPAM**

References

S1 M. Li, P. De, S. R. Gondi, B. S. Sumerlin, *J. Polym. Sci., Part A: Polymer Chemistry,* 2008, **46**, 5093-5100.

S2 X. Song, D. Hu, X. Yang, H. Zhang, W. Zhang, J. Li, M. Jia and Jihong Yu, *ACS Sustainable Chem. Eng*., 2019, **7**, 3624-3631.

S3 Y. Leng, J.-H. Wu, P.-P. Jiang and J. Wang, *Catal. Sci. Technol*., 2014, **4**, 1293-1300.